RESEARCH

Open Access

CrossMark

MHD mixed convection slip flow near a stagnation-point on a nonlinearly vertical stretching sheet

Ming Shen[1*], Fei Wang[1] and Hui Chen[2]

*Correspondence:
shenming0516@fzu.edu.cn
[1]College of Mathematics and
Computer Science, Fuzhou
University, Fuzhou, 350116, China
Full list of author information is
available at the end of the article

Abstract

The problem of magnetohydrodynamic (MHD) mixed convection flow near a stagnation-point region over a nonlinear stretching sheet with velocity slip and prescribed surface heat flux is investigated; this has not been studied before. Using a similarity transformation, the governing equations are transformed into a system of ordinary differential equations, and then are solved by employing a homotopy analysis method. The effects of the nonlinearity parameter, the magnetic field, mixed convection, suction/injection, and the boundary slip on the velocity and temperature profile are analyzed and discussed. The results reveal that the increasing exponent of the power-law stretching velocity increases the heat transfer rate at the surface. It is also found that the velocity slip and magnetic field increase the heat transfer rate when the free stream velocity exceeds the stretching velocity, *i.e.* $\varepsilon < 1$, and they suppress the heat transfer rate for $\varepsilon > 1$.

Keywords: stagnation-point flow; mixed convection; nonlinear stretching; slip

1 Introduction

The problem of stagnation-point flow and heat transfer on stretching sheet arises in an abundance of practical applications in industry and engineering, such as cooling of electronic devices and nuclear reactors, polymer extrusion, drawing of plastic sheets, *etc.*; and, moreover, in the magnetohydrodynamic (MHD) flow which has both liquid and magnetic properties and can exhibit particular characteristics in thermal conductivity. Thus the study of MHD stagnation-point flow on stretching sheet has attracted many researchers in recent times, and many problems are discussed as regards different aspects, including the stretching sheet with variable surface temperature [1] or viscous dissipation [2, 3], the effect of slip [4, 5], and the analysis of the unsteady case [6].

Different from the flow induced by a stretching horizontal sheet, the effect of mixed convection due to a buoyancy force could not be neglected for the vertical sheet. There has been increasing interest in studying the problem of MHD with mixed convection boundary layer flow and heat transfer characteristics over a stretching vertical surface [7–15]. Very recently, Ali *et al.* [16] studied the MHD mixed convection stagnation-point flow and heat transfer of an incompressible viscous fluid over a vertical stretching sheet, and the MHD boundary layer flow over a vertical stretching/shrinking sheet in a nano-fluid was investigated by Makinde *et al.* [17] and Das *et al.* [18].

The above investigations considered the flow on the linearly stretching sheet or vertical sheet, but the real stretching velocity does not always need to be linear or uniform. Some work has been done in this field. The similarity solution of the boundary layer equations for a nonlinearly stretching sheet has been found by Akyildiz *et al.* [19]. The flow and heat transfer over a nonlinearly stretching sheet has been investigated by Akyildiz and Siginer [20] by using a Legendre spectral method. Recently, Dhanai *et al.* [21], Ashraf *et al.* [22], and Mabood *et al.* [23] analyzed the boundary layer flow and heat transfer on a nonlinearly shrinking/stretching sheet immersed in a nanofluid.

In the present paper, motivated by the above studies, the problem of MHD mixed convection stagnation-point flow on the nonlinearly vertical stretching sheet is discussed in the presence of buoyancy force, suction/injection parameters, and boundary slip. The governing nonlinear coupled partial differential equations are reduced to a set of ordinary differential equations by means of similarity transformations. The reduced equations are solved by the homotopy analysis method (HAM) [24], which has been successfully applied to various interesting complicated fluid problems [25–30]. Graphs are plotted to gain physical insight toward the key embedding physical parameters. To the best of our knowledge, the series solutions for this model have not been presented before.

2 Mathematical formulation of the problem

We consider the steady two-dimensional MHD mixed convection flow in the vicinity of a stagnation point over a nonlinear stretching sheet with velocity slip and prescribed surface heat flux. The flow is confined to the region $y \geq 0$, where y is the coordinate measured normal to the stretching surface. A uniform magnetic field of strength is applied in the direction normal to the surface $y = 0$. The flow model along with the coordinate system is shown in Figure 1. It is assumed that the sheet stretching velocity $u_w(x) = cx^m$ and the external velocity is prescribed as $u_e(x) = ax^m$ where c and a are positive constants. The constant m is the nonlinearity parameter, with $m = 1$ for the linear case and $m \neq 1$ for the nonlinear case. Under the boundary layer approximation and the assumptions that the viscous dissipation and Joule heating are neglected, the basic equations of continuity, momentum, and energy are given by

$$\frac{\partial u}{\partial x} + \frac{\partial v}{\partial y} = 0, \tag{1}$$
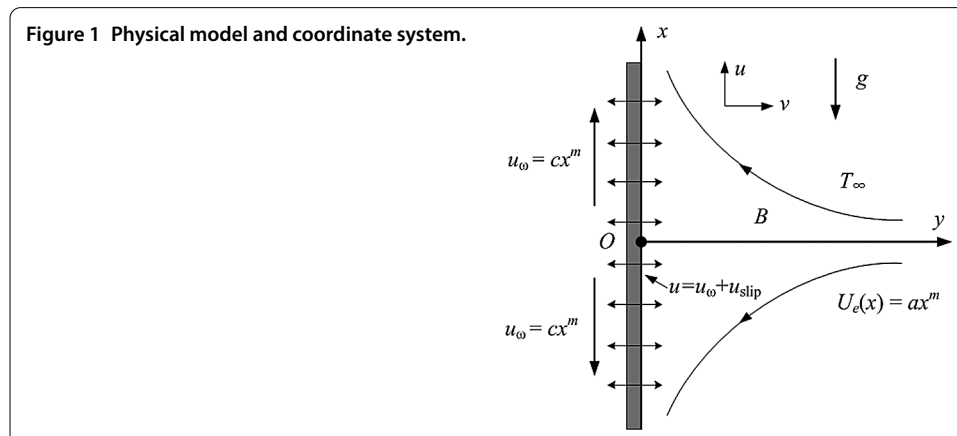

Figure 1 Physical model and coordinate system.

$$u\frac{\partial u}{\partial x} + v\frac{\partial u}{\partial y} = u_e\frac{du_e}{dx} + v\frac{\partial^2 u}{\partial y^2} + \frac{\sigma B^2(x)}{\rho}(u_e - u) + g\beta(T - T_\infty), \tag{2}$$

$$u\frac{\partial T}{\partial x} + v\frac{\partial T}{\partial y} = \alpha\frac{\partial^2 T}{\partial y^2}, \tag{3}$$

where u and v are the velocities in the x and y directions, v is the kinematic viscosity, ρ is the fluid density, σ is the electrical conductivity, $B(x)$ is the transverse magnetic field, g is the acceleration due to gravity, β is the thermal expansion coefficient, T is the fluid temperature, and α is the thermal diffusivity. The relevant boundary conditions are given by

$$u = u_w(x) + \frac{2 - \sigma_v}{\sigma_v}\lambda_0\frac{\partial u}{\partial y}, \qquad v = v_w(x), \qquad \frac{\partial T}{\partial y} = -\frac{q_w(x)}{k}, \quad \text{at } y = 0, \tag{4}$$

$$u \to u_e(x), \qquad T \to T_\infty \quad \text{as } y \to \infty, \tag{5}$$

where σ_v is the tangential momentum accommodation coefficient, λ_0 is the mean free path, $v_w(x)$ is the suction (injection) velocity, k is the thermal conductivity, and $q_w(x)$ is the surface heat flux.

We introduce the following similarity transformations:

$$\begin{cases} \eta = \sqrt{\frac{a}{v}}yx^{(m-1)/2}, \\ \psi = \sqrt{av}x^{(m+1)/2}f(\eta), \\ \theta = \sqrt{\frac{a}{v}}\frac{k(T-T_\infty)}{q_0 x^{2m-1}}. \end{cases} \tag{6}$$

Here ψ is the stream function. Equation (1) is satisfied by introducing ψ such that $u = \partial\psi/\partial y$ and $v = -\partial\psi/\partial x$. Employing the similarity variables (6), the velocity components u and v are given by

$$u = ax^m f'(\eta) \quad \text{and} \quad v = -\sqrt{av}x^{(m-1)/2}\left[\frac{m+1}{2}f(\eta) + \frac{m-1}{2}\eta f'(\eta)\right], \tag{7}$$

where the prime denotes differentiation with respect to η. To obtain similarity solutions, $B(x)$, $v_w(x)$, and $q_w(x)$ are taken as

$$B(x) = B_0 x^{(m-1)/2}, \qquad v_w = -\frac{\sqrt{av}(m+1)}{2}x^{(m-1)/2}S,$$

$$q_w(x) = q_0 x^{(5m-3)/2}, \tag{8}$$

where B_0, S, and q_0 are constants. It is noted that $S > 0$ corresponds to the injection case and $S < 0$ implies suction. Substituting (6) into (2) and (3), we get the following ordinary differential equations:

$$f''' + \frac{m+1}{2}ff'' + m(1 - f'^2) + M(1 - f') + \lambda\theta = 0, \tag{9}$$

$$\theta'' + \frac{P_r(m+1)}{2}f\theta' - P_r(2m-1)f'\theta = 0, \tag{10}$$

subject to the boundary conditions (4) and (5), which become

$$f(0) = S, \qquad f'(0) = \varepsilon + \delta f''(0), \qquad \theta'(0) = -1, \tag{11}$$

$$f'(\infty) = 1, \qquad \theta(\infty) = 0. \tag{12}$$

In the above equations, M is the magnetic parameter, λ is the mixed convection parameter, and P_r is the Prandtl number, and they are given by

$$M = \frac{\sigma B_0^2}{a\rho}, \qquad \lambda = \frac{g\beta q_0 \sqrt{\nu}}{ka^{5/2}} = \frac{Gr_x}{Re_x^{5/2}} \quad \text{and} \quad P_r = \frac{\nu}{\alpha} \tag{13}$$

with $Gr_x = g\beta q_w x^4 / k\nu^2$ and $Re_x = u_e x / \nu$ being the local Grashof and Reynolds numbers, respectively. It is noticed that λ is a constant with $\lambda < 0$ and $\lambda > 0$ corresponding to the opposing and assisting flows, respectively, while $\lambda = 0$ is for pure forced convection flow. Further, $\varepsilon = c/a$ is the velocity ratio parameter, and $\delta = (2 - \sigma_v)Kn_x Re_x^{1/2}/\sigma_v$ is the velocity slip parameter with the local Knudsen number $Kn_x = \lambda_0/\sqrt{\varepsilon}x$.

In addition, the quantities of practical interest in this study are the skin friction coefficient C_f and the local Nusselt number Nu_x, which are defined as

$$C_f = \frac{\tau_w(x)}{\rho u_e^2}, \qquad Nu_x = \frac{xq_w(x)}{k(T_w - T_\infty)}, \tag{14}$$

where the surface shear stress $\tau_w(x) = \mu(\partial u/\partial y)_{y=0}$ and $q_w(x)$ is the wall heat flux given by (8). Using the similarity variables (6), we obtain

$$Re_x^{1/2} C_f = f''(0), \qquad Re_x^{-1/2} Nu_x = 1/\theta(0). \tag{15}$$

3 Series solutions of HAM

In the framework of the HAM technique, we select the initial guesses and the linear operator as

$$f_0(\eta) = S + \eta + \frac{(\varepsilon - 1)}{2\delta + 1}\left(1 - \frac{1}{1 + \eta}\right), \qquad \theta_0(\eta) = \frac{1}{1 + \eta}, \tag{16}$$

$$\mathcal{L}_f = f''' + \frac{3}{1 + \eta}f'', \qquad \mathcal{L}_\theta = \theta'' + \frac{2}{1 + \eta}\theta', \tag{17}$$

where $\mathcal{L}_f$ and $\mathcal{L}_\theta$ satisfy

$$\mathcal{L}_f\left[C_1 + C_2\eta + \frac{C_3}{1 + \eta}\right] = 0, \tag{18}$$

$$\mathcal{L}_\theta\left[C_4 + \frac{C_5}{1 + \eta}\right] = 0, \tag{19}$$

in which C_i ($i = 1$-5) are arbitrary constants.

The zeroth order deformation equations are given by

$$(1 - q)\mathcal{L}_f\left[\bar{f}(\eta, q) - f_0(\eta)\right] = qh_f H_f(\eta)N_f\left[\bar{f}(\eta, q), \bar{\theta}[\eta, q]\right], \tag{20}$$

$$(1 - q)\mathcal{L}_\theta\left[\bar{\theta}(\eta, q) - \theta_0(\eta)\right] = qh_\theta H_\theta(\eta)N_\theta\left[\bar{f}(\eta, q), \bar{\theta}[\eta, q]\right], \tag{21}$$

and they satisfy the following boundary conditions:

$$\bar{f}(\eta,q) = S, \qquad \bar{f}'(\eta,q) = \varepsilon + \delta \bar{f}''(\eta,q), \qquad \bar{\theta}'(\eta,q) = -1, \quad \text{at } \eta = 0, \tag{22}$$

$$\bar{f}(\eta,q) \to 1, \qquad \bar{\theta}(\eta,q) \to 0 \quad \text{as } \eta \to \infty. \tag{23}$$

Here $q \in (0,1)$ is an embedding parameter and h_f and h_θ indicate the non-zero auxiliary parameters, $H_f(\eta)$ and $H_\theta(\eta)$ indicate the non-zero auxiliary functions, the nonlinear operators N_f, N_θ are defined as

$$N_f[\bar{f}(\eta,q), \bar{\theta}(\eta,q)] = \frac{\partial^3 \bar{f}(\eta,q)}{\partial \eta^3} + \frac{m+1}{2} \bar{f}(\eta,q) \frac{\partial^2 \bar{f}(\eta,q)}{\partial \eta^2}$$

$$+ m\left[1 - \left(\frac{\partial \bar{f}(\eta,q)}{\partial \eta}\right)^2\right] + M\left(1 - \frac{\partial \bar{f}(\eta,q)}{\partial \eta}\right)$$

$$+ \lambda \bar{\theta}(\eta,q), \tag{24}$$

$$N_\theta[\bar{f}(\eta,q), \bar{\theta}(\eta,q)] = \frac{\partial^2 \bar{\theta}(\eta,q)}{\partial \eta^2} + \frac{P_r(m+1)}{2} \bar{f}(\eta,q) \frac{\partial \bar{\theta}(\eta,q)}{\partial \eta}$$

$$- P_r(2m-1) \bar{\theta}(\eta,q) \frac{\partial \bar{f}(\eta,q)}{\partial \eta}. \tag{25}$$

For $q = 0$ and $q = 1$, we have

$$\bar{f}(\eta,0) = f_0(\eta), \qquad \bar{f}(\eta,1) = f(\eta), \tag{26}$$

$$\bar{\theta}(\eta,0) = \theta_0(\eta), \qquad \bar{\theta}(\eta,1) = \theta(\eta). \tag{27}$$

By using a Taylor series, it is easy to obtain

$$\bar{f}(\eta,q) = f_0(\eta) + \sum_{n=1}^{\infty} f_n(\eta) q^n, \tag{28}$$

$$\bar{\theta}(\eta,q) = \theta_0(\eta) + \sum_{n=1}^{\infty} \theta_n(\eta) q^n, \tag{29}$$

in which

$$f_n(\eta) = \frac{1}{n!} \frac{\partial^n \bar{f}(\eta,q)}{\partial q^n}\bigg|_{q=0}, \qquad \theta_n(\eta) = \frac{1}{n!} \frac{\partial^n \bar{\theta}(\eta,q)}{\partial q^n}\bigg|_{q=0}. \tag{30}$$

The parameters h_f and h_θ are properly selected such that series solutions converge at $p = 1$. Substituting $p = 1$ into (28)-(29) gives

$$f(\eta) = f_0(\eta) + \sum_{n=0}^{\infty} f_n(\eta), \tag{31}$$

$$\theta(\eta) = \theta_0(\eta) + \sum_{n=0}^{\infty} \theta_n(\eta). \tag{32}$$

Then the mth order deformation equations and boundary conditions are

$$\mathcal{L}_f\big[f_n(\eta) - \chi_n f_{n-1}(\eta)\big] = h_f H_f(\eta)\mathfrak{R}_n^f(\eta), \tag{33}$$

$$\mathcal{L}_\theta\big[\theta_n(\eta) - \chi_n \theta_{n-1}(\eta)\big] = h_\theta H_\theta(\eta)\mathfrak{R}_n^\theta(\eta), \tag{34}$$

$$f_n(0) = f_n'(0) - \delta f_n''(0) = f_n'(\infty) = 0, \qquad \theta_n'(0) = \theta_n(\infty) = 0, \tag{35}$$

$$\mathfrak{R}_n^f(\eta) = f_{n-1}''' - M f_{n-1}' + \lambda \theta_{n-1} + \frac{m+1}{2}\sum_{k=0}^{n-1} f_{n-1-k}f_k''$$

$$- m \sum_{k=0}^{n-1} f_{n-1-k}' f_k' + (M+m)(1-\chi_n), \tag{36}$$

$$\mathfrak{R}_n^\theta(\eta) = \theta_{n-1}'' + \frac{P_r(m+1)}{2}\sum_{k=0}^{n-1} f_{n-1-k}\theta_k' - P_r(2m-1)\sum_{k=0}^{n-1} f_{n-1-k}'\theta_k \tag{37}$$

with

$$\chi_n = \begin{cases} 0, & n \le 1, \\ 1, & n \ge 1. \end{cases} \tag{38}$$

The general solutions of (33)-(35) are

$$f_n(\eta) = \tilde{f}_n(\eta) + C_1 + C_2\eta + \frac{C_3}{1+\eta}, \tag{39}$$

$$\theta_n(\eta) = \tilde{\theta}_n(\eta) + C_4 + \frac{C_5}{1+\eta}, \tag{40}$$

where $\tilde{f}_n(\eta)$ and $\tilde{\theta}_n(\eta)$ are the special solutions of the mth order deformation equations and C_i ($i = 1\text{-}5$) are governed by the boundary conditions (35), which are given by

$$C_2 = C_4 = 0, \qquad C_1 = -C_3 - \tilde{f}_n(0), \qquad C_3 = \frac{\tilde{f}_n'(0) - \delta\tilde{f}_n''(0)}{1+2\delta}, \qquad C_5 = \tilde{\theta}_n'(0). \tag{41}$$

For simplicity, here we take $\hbar_f = \hbar_\theta = \hbar$. In addition, according to the rule of the solution expression and the mth order deformation equation, the auxiliary functions $H_f(\eta)$ and $H_\theta(\eta)$ are chosen in the form
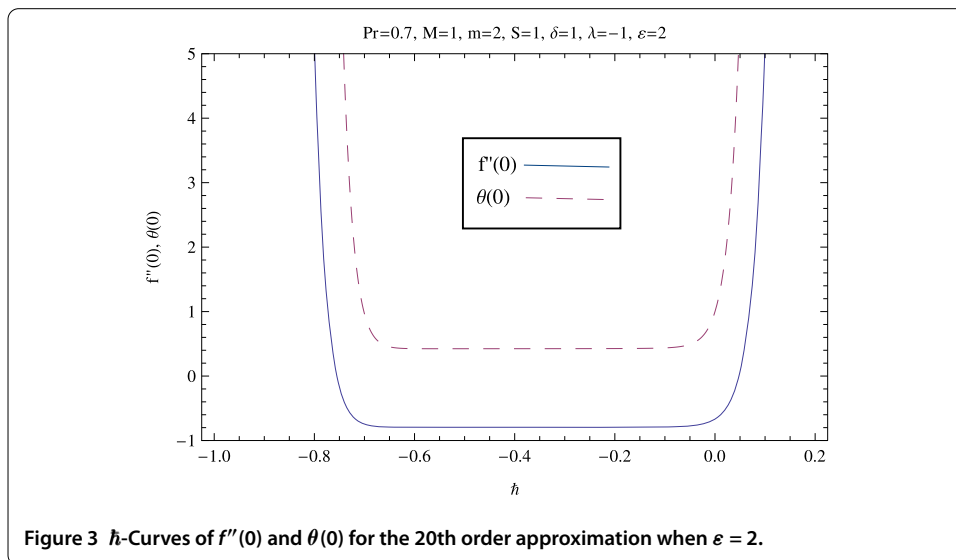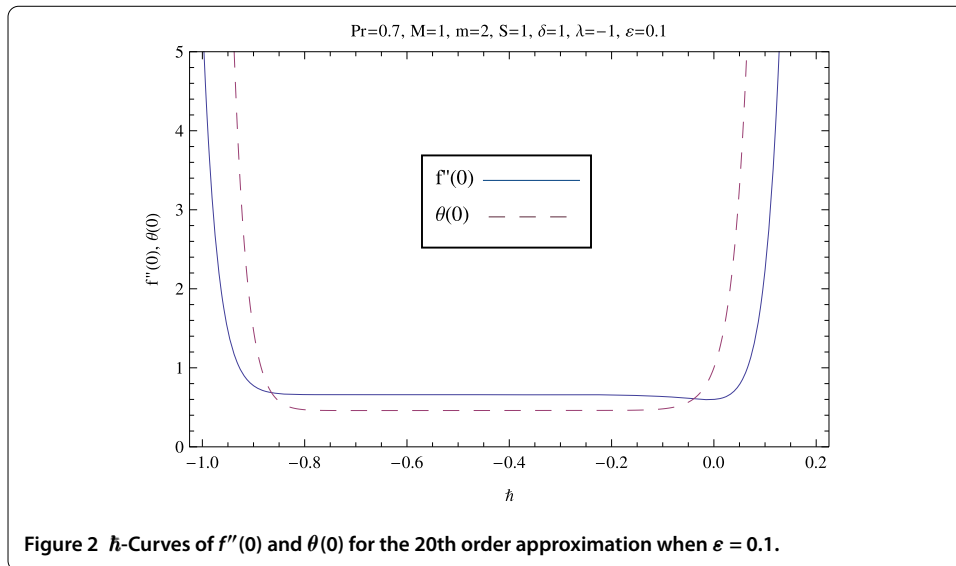
$$H_f(\eta) = \frac{1}{(1+\eta)^4}, \qquad H_\theta(\eta) = \frac{1}{(1+\eta)^3}. \tag{42}$$

By employing the software MATHEMATICA, (33) and (34) can be solved one after the other in the order $n = 1, 2, 3, \ldots$.

4 Analysis of the results
4.1 Convergence of the solutions
In order to ensure the convergence of the obtained series solutions, it is necessary to choose the appropriate range for the auxiliary parameter $\hbar$. As pointed out by Liao [24], the interval for the admissible values for $\hbar$ corresponds to line segments nearly parallel to

Figure 2 $\hbar$**-Curves of $f''(0)$ and $\theta(0)$ for the 20th order approximation when $\varepsilon = 0.1$.**

Figure 3 $\hbar$**-Curves of $f''(0)$ and $\theta(0)$ for the 20th order approximation when $\varepsilon = 2$.**

the horizontal axis. Figures 2 and 3 are plotted to show the admissible values of $\hbar$ for the function $f''(0)$ and $\theta(0)$ at 20th order approximation. To ensure the convergence of the series solution by HAM, it is observed from Figures 2 and 3 that the value of $\hbar$ should be chosen from $-0.6 \leq \hbar \leq -0.1$.

From the computation, it is found that the series solutions (31) and (32) converge in the whole region of η when we take $\hbar = -0.5$. Table 1 shows the convergence of the solutions for different orders of approximations when $Pr = 0.7$, $M = 1$, $m = 2$, $S = 1$, $\lambda = -1$, and $\delta = 1$. In order to further validate the present results, we show a comparison with previous work in Table 2. The results indicate that the numerical and analytical solutions are in good agreement. Hence we are confident that our results are accurate.

4.2 Results and discussion

The influence of key parameters on the coefficient of skin friction, the local Nusselt number, the velocity, and the temperature profiles are shown in this section. Figures 4 and 5

Table 1 Values of f''(0) and 1/θ(0) for different orders of approximations

Order of approximation	(a) ε = 0.1		(b) ε = 1		(c) ε = 2	
	f''(0)	1/θ(0)	f''(0)	1/θ(0)	f''(0)	1/θ(0)
1	0.5878	1.8038	−0.0556	2.1622	−0.7858	2.7746
5	0.6511	2.1674	−0.0283	2.2484	−0.7940	2.3482
10	0.6591	2.1700	−0.0252	2.2587	−0.7943	2.3501
15	0.6597	2.1736	−0.0248	2.2635	−0.7944	2.3559
20	0.6598	2.1758	−0.0248	2.2657	−0.7944	2.3580
25	0.6599	2.1768	−0.0248	2.2666	−0.7944	2.3589
30	0.6599	2.1771	−0.0248	2.2670	−0.7945	2.3593
35	0.6599	2.1772	−0.0248	2.2670	−0.7945	2.3593
40	0.6599	2.1772	−0.0248	2.2670	−0.7945	2.3593

Table 2 Values of f''(0) and 1/θ(0) for different orders of approximations

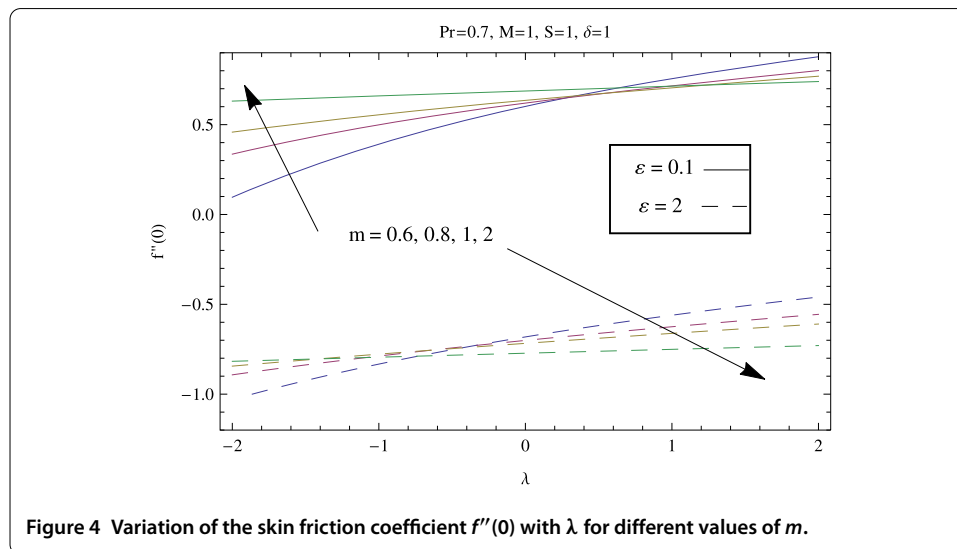| 40th order of approximation	Yacob and Ishak [31]		Present results	
Pr	f''(0)	1/θ(0)	f''(0)	1/θ(0)
0.7	1.8339	0.7776	1.8337	0.7771
1	1.7338	0.8780	1.7337	0.8780

Figure 4 Variation of the skin friction coefficient f''(0) with λ for different values of m.

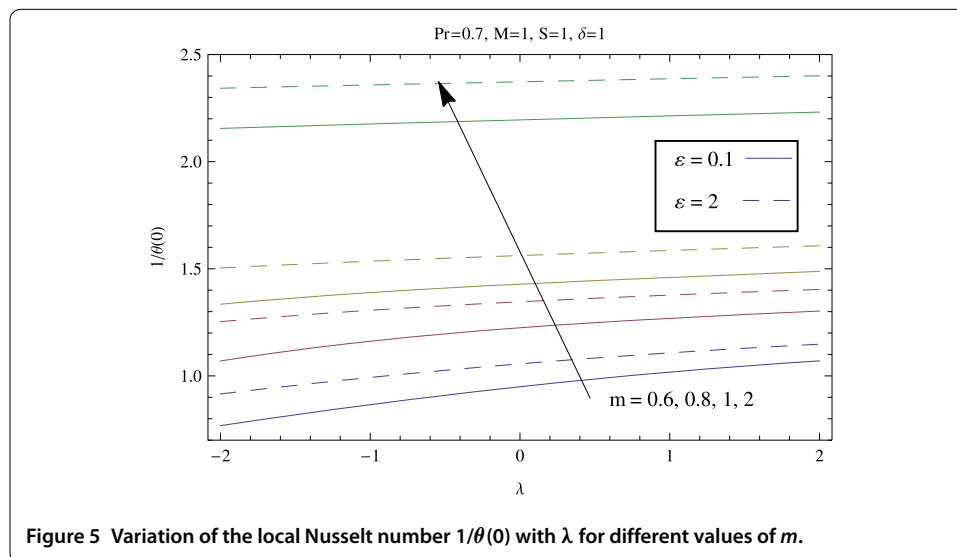**Figure 5 Variation of the local Nusselt number 1/θ(0) with λ for different values of m.**

present the variation of the skin friction coefficient $f''(0)$ and the local Nusselt number $1/\theta(0)$ with mixed convection parameter λ. The results show that the values of $f''(0)$ and $1/\theta(0)$ increase with λ. It is also observed from Figure 4 that the values of $f''(0)$ are negative for $\varepsilon = 2 > 1$, which means that the sheet exerts a drag force on the fluid. For $\varepsilon = 0.1 < 1$, the values of $f''(0)$ become positive, which indicates that the formation of the boundary layer does not depend solely on the stretching sheet. On the other hand, the values of $1/\theta(0)$, which represents the heat transfer rate at the surface, increase with the nonlinearity parameter m and they are always positive, *i.e.* the heat is transferred from the hot sheet to the cold fluid.

The effects of mixed convection parameter λ on the velocity and temperature profiles are shown in Figures 6 and 7. The flow has a boundary layer structure, while the velocity ratio parameter $\varepsilon < 1$ and the nonlinearity parameter $m \geq 1$. On the other hand, when $\varepsilon > 1$ and $m \geq 1$, the flow has an inverted boundary layer structure which results from the fact
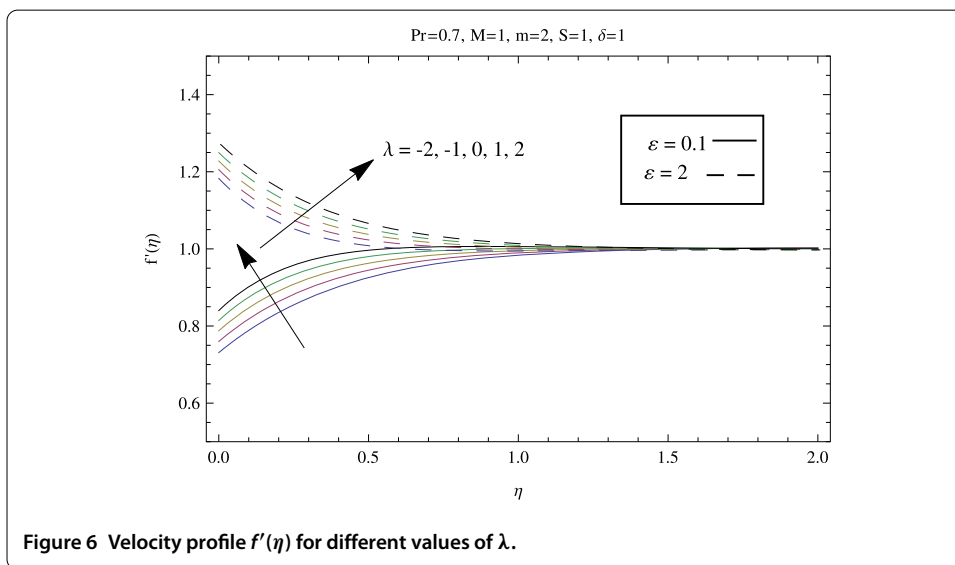
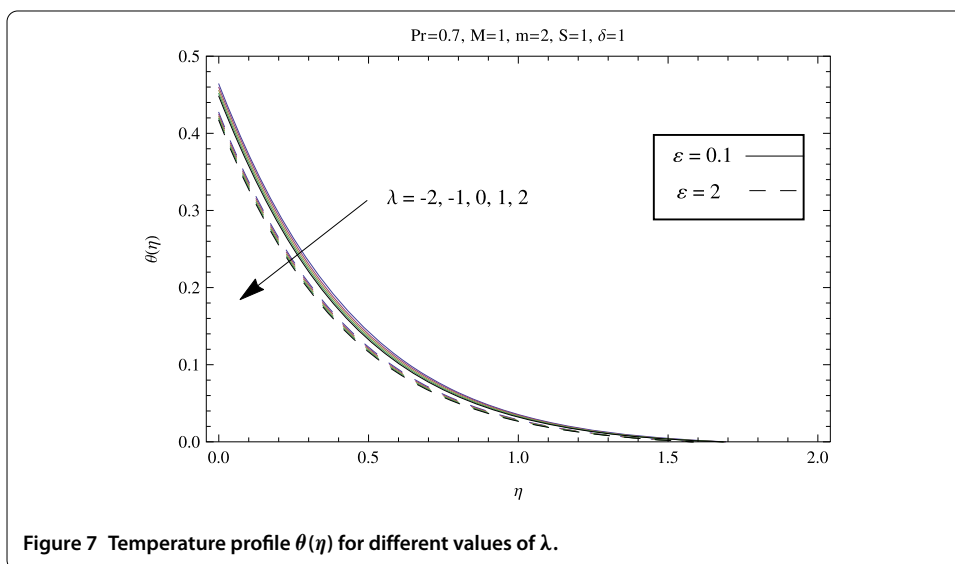**Figure 6 Velocity profile $f'(\eta)$ for different values of λ.**

Figure 7 Temperature profile $\theta(\eta)$ for different values of λ.

that the stretching velocity $u_w(x)$ of the surface exceeds the velocity $u_e(x)$ of the external stream. From Figure 6, it is observed that the thickness of the velocity boundary layer decreases with λ for $\varepsilon = 0.1 < 1$, but it increases as λ increases for $\varepsilon = 2 > 1$. The velocity field $f'(\eta)$ is always an increasing function of λ for the two cases. Figure 7 shows that an increase in λ corresponds to a decrease in the temperature and the thermal boundary layer thickness. From this figure, we can see that the wall temperature $\theta(0)$ also decreases with increasing λ, which means that the heat transfer rate $1/\theta(0)$ increases as λ increases. It is worth pointing out here that the temperature profiles show less deviation for different values of λ.
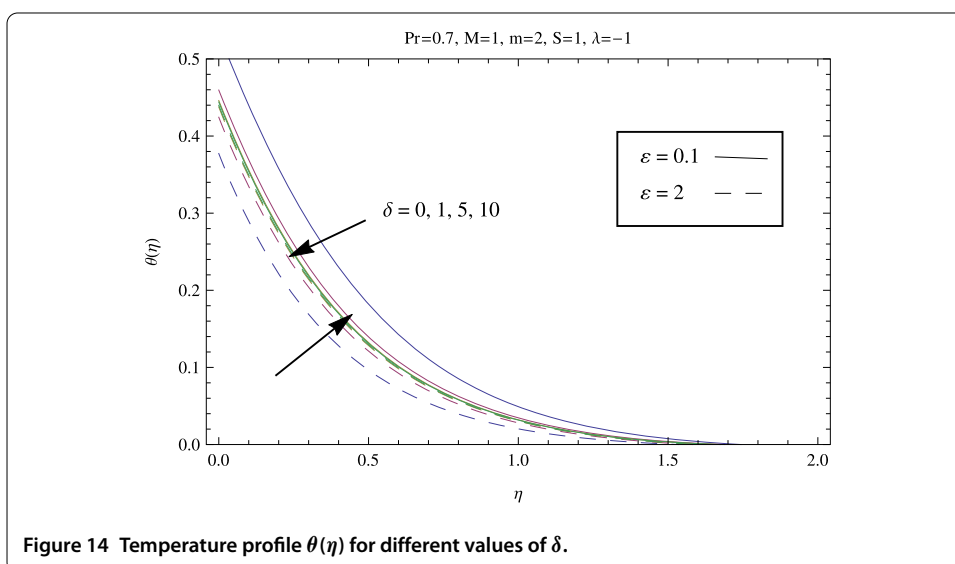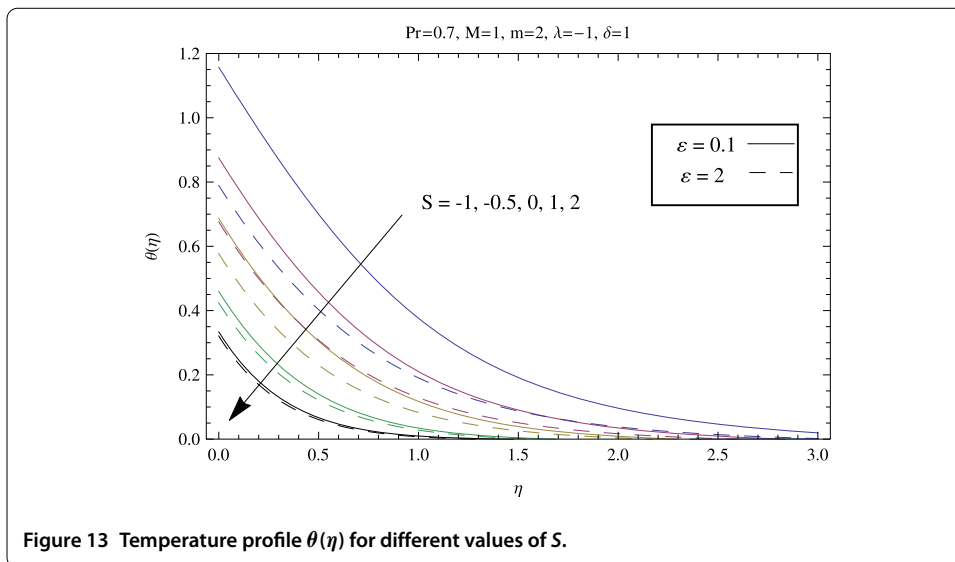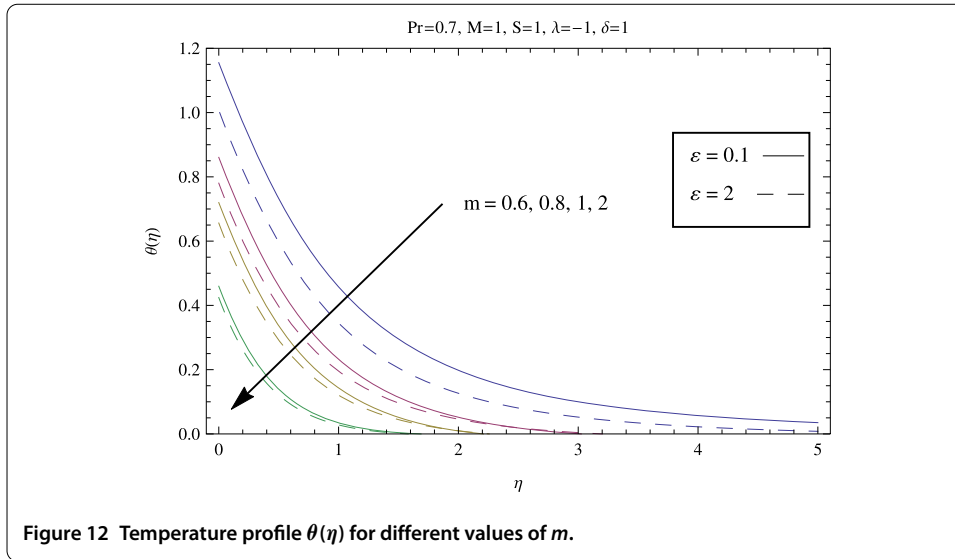
Figures 8-11 illustrate the effects of m, S, δ, and M on the velocity profiles for the two cases of $\varepsilon < 1$ and $\varepsilon > 1$. It is observed that the thickness of the velocity boundary layer decreases with increasing values of m, S, δ, and M for both cases, which implies an increasing magnitude of the velocity gradient at the surface. Thus, the skin friction coefficient $f''(0)$
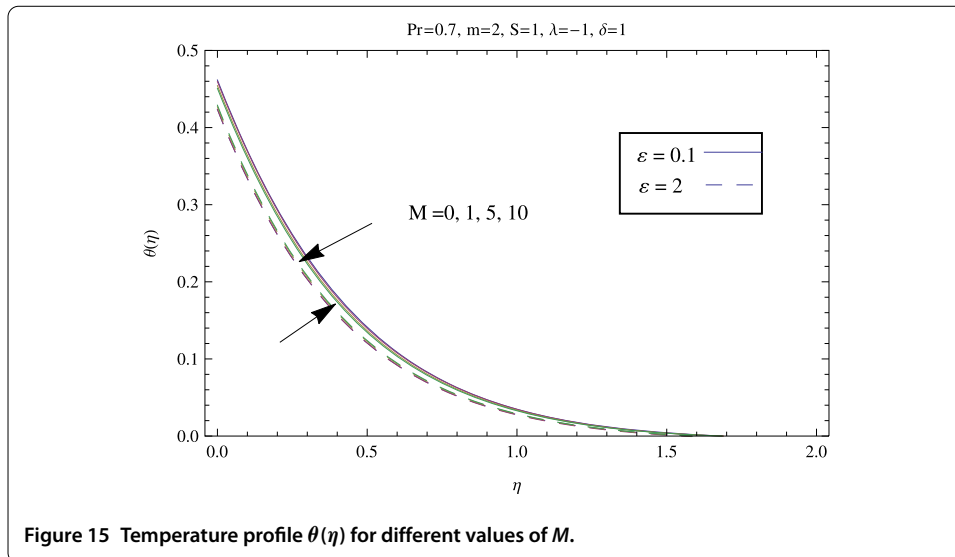

Figure 8 Velocity profile $f'(\eta)$ for different values of m.

Figure 9 Velocity profile $f'(\eta)$ for different values of S.

Figure 10 Velocity profile $f'(\eta)$ for different values of δ.

Figure 11 Velocity profile $f'(\eta)$ for different values of M.
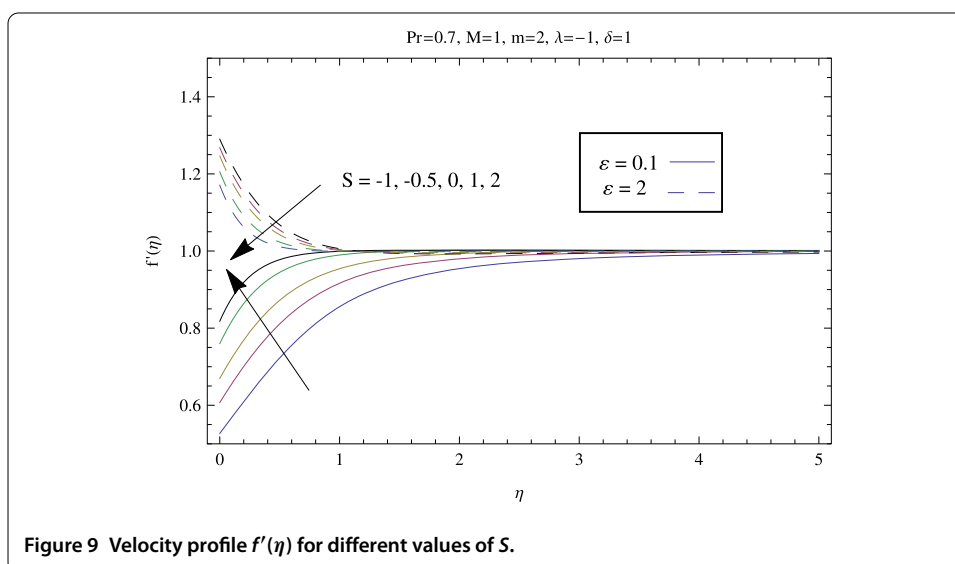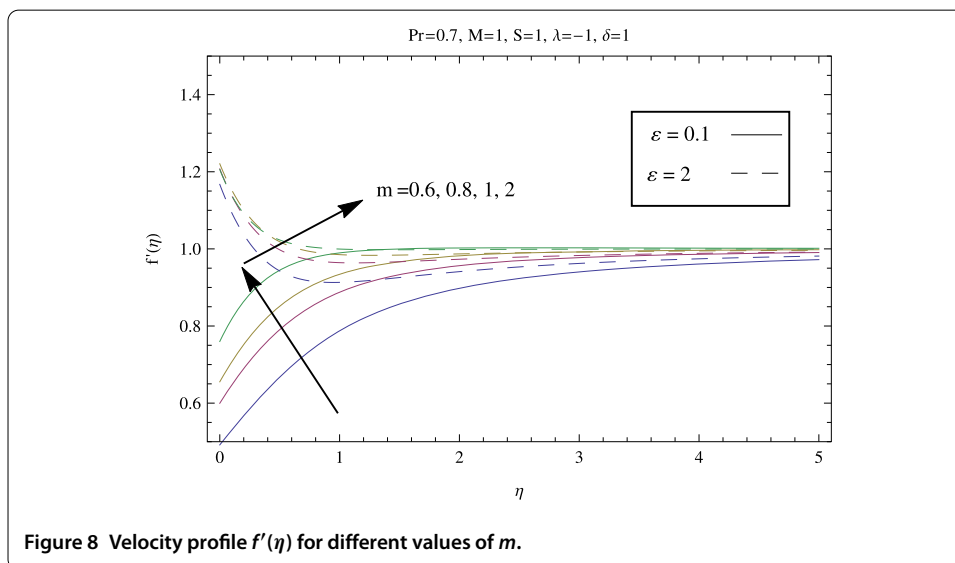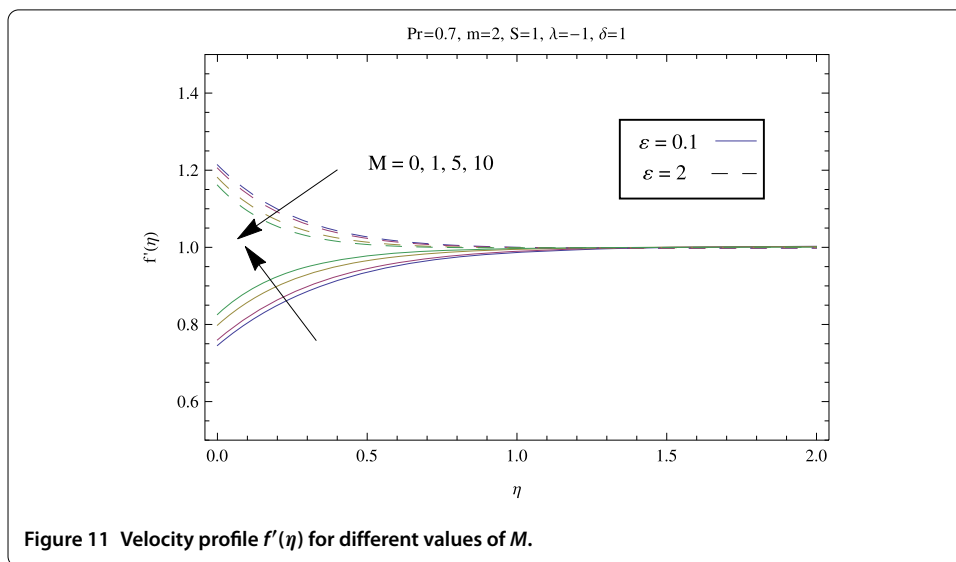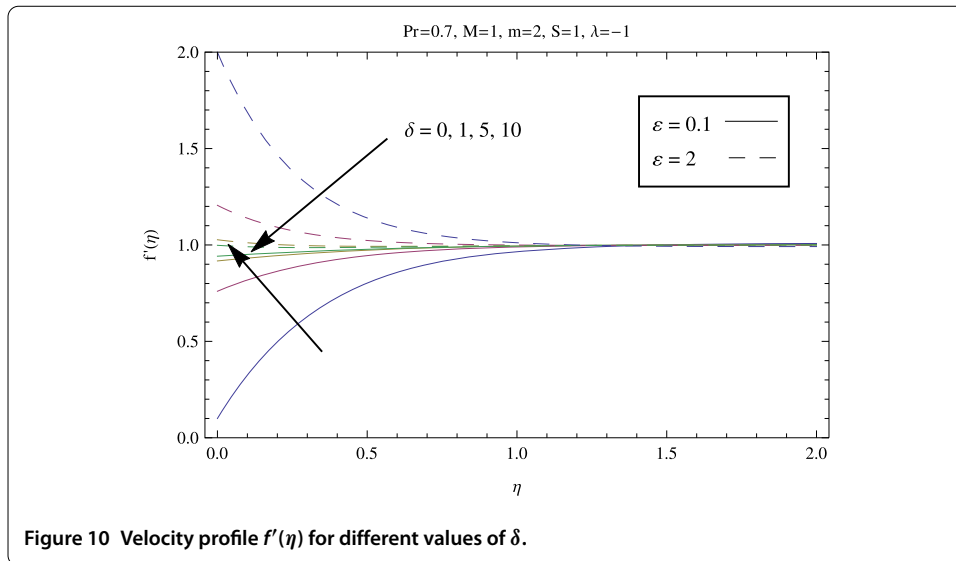
increases with the increasing values of m, S, δ, and M. From a physical point of view this follows from the fact that with a rise in the strength of magnetic parameter M, the Lorentz force associated with the magnetic field makes the boundary layer thinner. Further, it is seen from Figures 9-11 that the velocity inside the velocity boundary layer increases with S, δ, and M for $\varepsilon < 1$ but decreases with these parameters for $\varepsilon > 1$. In addition, it is indicated that the velocity slip parameter has a significant influence on the velocity compared to the parameters m, S, and M.

Figures 12-15 show the temperature profiles for selected values of the parameters m, S, δ, and M for the two cases of $\varepsilon < 1$ and $\varepsilon > 1$. The temperature is found to decrease to zero monotonically as η increases, which satisfies the far field boundary condition $\theta(\infty) = 0$. The results display that the temperature and thickness of the thermal boundary layer is lower for $\varepsilon = 2$ and higher for $\varepsilon = 0.1$ when the other parameters are constant. Figures 12 and 13 show that the wall temperature $\theta(0)$ decreases with increasing m, S for the two cases. Thus, the heat transfer rate at the surface increases as m and S increase. Further-

Pr=0.7, M=1, S=1, λ=−1, δ=1

$\varepsilon = 0.1$ ———

$\varepsilon = 2$ − − −

m = 0.6, 0.8, 1, 2

Figure 12 Temperature profile $\theta(\eta)$ for different values of m.

Pr=0.7, M=1, m=2, λ=−1, δ=1

$\varepsilon = 0.1$ ———

$\varepsilon = 2$ − − −

S = -1, -0.5, 0, 1, 2

Figure 13 Temperature profile $\theta(\eta)$ for different values of S.

Pr=0.7, M=1, m=2, S=1, λ=−1

$\varepsilon = 0.1$ ———

$\varepsilon = 2$ − − −

δ = 0, 1, 5, 10

Figure 14 Temperature profile $\theta(\eta)$ for different values of δ.

Figure 15 Temperature profile $\theta(\eta)$ for different values of M.

more, it is easy to see that the temperature and thickness of thermal boundary layer also decrease with increasing these two parameters. Different characteristics are observed in Figures 14 and 15. The wall temperature and thickness of thermal boundary layer decrease with increasing δ and M for $\varepsilon < 1$, and the reverse trend is observed for the case of $\varepsilon > 1$. Thus, the heat transfer rate at the surface increases with δ or M for $\varepsilon < 1$, and the opposite behaviors are observed for the effects of δ and M for $\varepsilon > 1$.

5 Conclusions

In this work, the MHD mixed convection stagnation-point flow toward a nonlinearly stretching vertical sheet is analyzed. Different from the previous works, the current results focus on the effect of nonlinearly vertical stretching for the MHD stagnation-point flow with mixed convection. The analytic solutions for momentum and energy equations have been obtained by the method of HAM. The main conclusions can be summarized as follows.

- The increase of nonlinearity parameter m leads to an increases of the heat transfer rate at surface $1/\theta(0)$, and to a decrease of both the thicknesses of the velocity and the thermal boundary layer.
- The coefficient of the skin friction $f''(0)$ and the heat transfer rate at the surface $1/\theta(0)$ increase with increasing mixed convection parameter λ.
- The heat transfer rate increases as the velocity slip parameter δ and magnetic parameter M increase for $\varepsilon < 1$, but it decreases with these two parameters for $\varepsilon > 1$.
- Inside the velocity boundary layer, the velocity increases with the increasing S, δ, and M for $\varepsilon < 1$, and the opposite trend is displayed for $\varepsilon > 1$.
- Inside the thermal boundary layer, the temperature always decreases with increasing λ, m, and S.

Author details
[1]College of Mathematics and Computer Science, Fuzhou University, Fuzhou, 350116, China. [2]School of Mechanical Engineering and Automation, Fuzhou University, Fuzhou, 350116, China.

References
1. Ishak, A, Jafar, K, Nazar, R, Pop, I: MHD stagnation point flow towards a stretching sheet. Physica A **388**(13), 3377-3383 (2009)
2. Khan, ZH, Khan, WA, Qasim, M, Shah, IA: MHD stagnation point ferrofluid flow and heat transfer toward a stretching sheet. IEEE Trans. Nanotechnol. **13**(1), 35-40 (2014)
3. Shateyi, S, Makinde, OD: Hydromagnetic stagnation-point flow towards a radially stretching convectively heated disk. Math. Probl. Eng. **2013**, Article ID 616947 (2013)
4. Aman, F, Ishak, A, Pop, I: Magnetohydrodynamic stagnation-point flow towards a stretching/shrinking sheet with slip effects. Int. Commun. Heat Mass Transf. **47**, 68-72 (2013)
5. Singh, G, Makinde, OD: MHD slip flow of viscous fluid over an isothermal reactive stretching sheet. Ann. Fac. Eng. Hunedoara Int. J. Eng. **11**(2), 41-46 (2013)
6. Shateyi, S, Marewo, GT: Numerical analysis of unsteady MHD flow near a stagnation point of a two-dimensional porous body with heat and mass transfer, thermal transfer, and chemical reaction. Bound. Value Probl. **2014**, 218 (2014)
7. Ishak, A, Nazar, R, Pop, I: MHD mixed convection boundary layer flow towards a stretching vertical surface with constant wall temperature. Int. J. Heat Mass Transf. **53**(23-24), 5330-5334 (2010)
8. Kumari, M, Nath, G: Unsteady MHD mixed convection flow over an impulsively stretched permeable vertical surface in a quiescent fluid. Int. J. Non-Linear Mech. **45**(3), 310-319 (2010)
9. Ali, FM, Nazar, R, Arifin, NM, Pop, I: Effect of Hall current on MHD mixed convection boundary layer flow over a stretched vertical flat plate. Meccanica **46**(5), 1103-1112 (2011)
10. Hayat, T, Qasim, M: Radiation and magnetic field effects on the unsteady mixed convection flow of a second grade fluid over a vertical stretching sheet. Int. J. Numer. Methods Fluids **66**(7), 820-832 (2011)
11. Turkyilmazoglu, M: The analytical solution of mixed convection heat transfer and fluid flow of a MHD viscoelastic fluid over a permeable stretching surface. Int. J. Mech. Sci. **77**, 263-268 (2013)
12. Chamkha, AJ, El-Kabeir, S: Unsteady heat and mass transfer by MHD mixed convection flow over an impulsively stretched vertical surface with chemical reaction and Soret and Dufour effects. Chem. Eng. Commun. **200**(9), 1220-1236 (2013)
13. Hassanien, IA, El-Hawary, HM, Mahmoud, MAA: Thermal radiation effect on flow and heat transfer of unsteady MHD micropolar fluid over vertical heated nonisothermal stretching surface using group analysis. Appl. Math. Mech. **34**(6), 703-720 (2013)
14. Shateyi, S: A new numerical approach to MHD flow of a Maxwell fluid past a vertical stretching sheet in the presence of thermophoresis and chemical reaction. Bound. Value Probl. **2013**, 196 (2013)
15. Makinde, OD: Heat and mass transfer by MHD mixed convection stagnation point flow toward a vertical plate embedded in a highly porous medium with radiation and internal heat generation. Meccanica **47**, 1173-1184 (2012)
16. Ali, FM, Nazar, R, Arifin, NM, Pop, I: Mixed convection stagnation-point flow on vertical stretching sheet with external magnetic field. Appl. Math. Mech. **35**(2), 155-166 (2014)
17. Makinde, OD, Khan, AH, Khan, ZH: Buoyancy effects on MHD stagnation point flow and heat transfer of a nanofluid past a convectively heated stretching/shrinking sheet. Int. J. Heat Mass Transf. **62**, 526-533 (2013)
18. Das, S, Jana, RN, Makinda, OD: MHD boundary layer slip flow and heat transfer of nanofluid past a vertical stretching sheet with non-uniform heat generation/absorption. Int. J. Nanosci. **13**(3), 1450019 (2014)
19. Akyildiz, FT, Siginer, DA, Vajravelu, K, Cannon, JR, Van Gorder, RA: Similarity solutions of the boundary layer equations for a nonlinearly stretching sheet. Math. Methods Appl. Sci. **33**(5), 601-606 (2010)
20. Akyildiz, FT, Siginer, DA: Galerkin-Legendre spectral method for the velocity and thermal boundary layers over a non-linearly stretching sheet. Nonlinear Anal., Real World Appl. **11**(2), 735-741 (2010)
21. Dhanai, R, Rana, P, Kumar, L: Multiple solutions of MHD boundary layer flow and heat transfer behavior of nanofluids induced by a power-law stretching/shrinking permeable sheet with viscous dissipation. Powder Technol. **273**, 62-70 (2015)
22. Ashraf, MB, Hayat, T, Alsaedi, A: Three-dimensional flow of Eyring-Powell nanofluid by convectively heated exponentially stretching sheet. Eur. Phys. J. Plus **130**(1), 1-16 (2015)
23. Mabood, F, Khan, WA, Ismail, AIM: MHD boundary layer flow and heat transfer of nanofluids over a nonlinear stretching sheet: a numerical study. J. Magn. Magn. Mater. **374**, 569-576 (2015)
24. Liao, S: Beyond Perturbation: Introduction to the Homotopy Analysis Method. CRC Press, Boca Raton (2003)
25. Rashidi, MM, Pour, SAM: Analytic approximate solutions for unsteady boundary-layer flow and heat transfer due to a stretching sheet by homotopy analysis method. Nonlinear Anal., Model. Control **15**(1), 83-95 (2010)
26. Nadeem, S, Mehmood, R, Akbar, NS: Non-orthogonal stagnation point flow of a nano non-Newtonian fluid towards a stretching surface with heat transfer. Int. J. Heat Mass Transf. **57**(2), 679-689 (2013)
27. Hayat, T, Iqbal, Z, Mustafa, M, Alsaedi, A: Stagnation-point flow of Jeffrey fluid with melting heat transfer and Soret and Dufour effects. Int. J. Numer. Methods Heat Fluid Flow **24**(2), 402-418 (2014)

28. Hayat, T, Farooq, M, Alsaedi, A: Melting heat transfer in the stagnation-point flow of Maxwell fluid with double-diffusive convection. Int. J. Numer. Methods Heat Fluid Flow **24**(3), 760-774 (2014)
29. Hayat, T, Iqbal, Z, Mustafa, M, Alsaedi, A: Unsteady flow and heat transfer of Jeffrey fluid over a stretching sheet. Therm. Sci. **18**(4), 1069-1078 (2014)
30. Mabood, F, Khan, WA: Approximate analytic solutions for influence of heat transfer on MHD stagnation point flow in porous medium. Comput. Fluids **100**, 72-78 (2014)
31. Yacob, NA, Ishak, A: MHD flow of a micropolar fluid towards a vertical permeable plate with prescribed surface heat flux. Chem. Eng. Res. Des. **89**(11), 2291-2297. (2011)